

KALMAN FILTER BASED SYSTEM IDENTIFICATION EXPLOITING THE DECORRELATION EFFECTS OF LINEAR PREDICTION

Stefan Kühl, Christiane Antweiler, Tobias Hübschen, Peter Jax

Institute of Communication Systems (IKS)
RWTH Aachen University, Germany

ABSTRACT

In system identification one problem is the autocorrelation of the excitation signal which often crucially affects the adaptation process. This paper focuses on the Kalman filter based adaptation working in the frequency domain and the implication due to correlated signal input. Principle simulations and the introduction of a reference model indicate to which extent correlation take effect. The experimental results demonstrate that even though the Kalman approach already takes advantage from a certain level of inherent decorrelation, it also benefits from additional decorrelation. To address this issue, we derive a new realizable efficient structure combining the Kalman filter based adaptation with linear prediction techniques. The performance gains of the proposed approach are confirmed via experiments for an acoustic echo cancellation application for different scenarios.

Index Terms— System identification, Kalman filter, linear prediction, decorrelation, acoustic echo cancellation.

1. INTRODUCTION

The problem of single-channel system identification, such as needed for acoustic echo cancellation (AEC) or active noise control (ANC), has been investigated for several decades. Least mean square (LMS) based algorithms are cost-beneficial solutions in terms of complexity, simplicity and performance [1–3]. However, for a robust performance accurate control mechanisms are required [4, 5]. In addition, the LMS algorithm suffers severely from correlated excitation signals. This problem has been counteracted, e.g., by the introduction of decorrelation filters in the adaptation process [6–11] or projection algorithms [12–14]. Recently, more and more solutions rely on Kalman filter based adaptation in the time domain [15, 16] or frequency domain [17, 18]. The Kalman filter is the optimal linear solution in terms of a minimum mean square error criterion. It is of special interest that the LMS algorithm with perfect stepsize control can be interpreted as a special case of the Kalman filter [19]. This strong relation between the Kalman filter and the LMS algorithm leads us to the questions, whether correlation affects the Kalman filter based adaptation and to which extent we could improve the performance introducing, in analogy to [6, 7, 9], an additional decorrelation stage into the adaptation process. It is well understood that these two questions gain even more importance extending the Kalman identification problem in a next step to multi-channel systems.

The paper is structured as follows. In Sec. 2, the Kalman filter according to [17, 18] is reviewed and the influence of the correlation on the adaptation is shown for different excitation signals. Within a reference experiment the influence of a decorrelation stage prior to the adaptation and transmission is investigated in Sec. 3. Afterwards in Sec. 4 a new, realizable algorithm is proposed combining the conventional Kalman filter with linear prediction. Furthermore, the

new algorithm is analyzed in terms of complexity. Finally, in Sec. 5 simulation results for different conditions are compared and evaluated in the context of an AEC application.

2. FREQUENCY DOMAIN KALMAN FILTER

Figure 1 shows the principle block diagram of the system identification approach using Kalman filtering. The excitation signal and

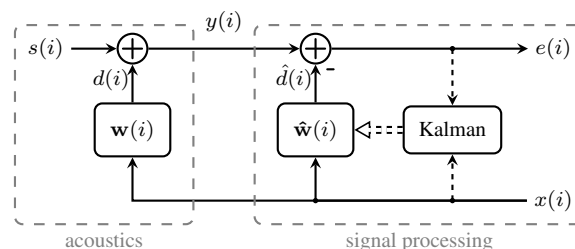


Fig. 1. System identification with Kalman filter

measurement noise signal are denoted by $x(i)$ and $s(i)$, respectively, with the time index i . The impulse response of the unknown system is represented by the vector $\mathbf{w}(i)$. In contrast to scalars, in the following, vectors and matrices are denoted by boldface letters. In the subsequent simulations, a finite length L of the impulse response is presumed, so that it can be represented by

$$\mathbf{w}(i) = (w_1(i), w_2(i), \dots, w_L(i))^T, \quad (1)$$

where $(\cdot)^T$ denotes the transpose of a vector. The system response $d(i)$ can be expressed by the inner product $d(i) = \mathbf{x}^T(i) \mathbf{w}(i)$ with the excitation vector

$$\mathbf{x}(i) = (x(i), x(i-1), \dots, x(i-L+1))^T. \quad (2)$$

The measured signal is denoted by $y(i)$. The adaptive filter is represented by the vector $\hat{\mathbf{w}}(i)$ of length L and the estimate of the system response by $\hat{d}(i)$. The difference $e(i) = y(i) - \hat{d}(i)$ refers to the resulting error signal.

As basic identification algorithm, the *diagonalized* Kalman filter adaptation in the frequency domain with an overlap-save framework is used [17, 18]. The processing is performed in frames of length M with frameshift R where k denotes the frame index. Furthermore, the vectors

$$\begin{aligned} \mathbf{x}_M(k) &= (x(kR - M + 1), x(kR - M + 2), \dots, x(kR))^T \\ \mathbf{y}_R(k) &= (y(kR - R + 1), y(kR - R + 2), \dots, y(kR))^T, \end{aligned} \quad (3)$$

the Fourier-matrix \mathbf{F}_M of size $M \times M$, and the zero-padding matrix $\mathbf{Q}_R = (\mathbf{0}_{M-R} \ \mathbf{I}_R)^T$ of size $M \times R$ are defined with the identity-matrix \mathbf{I}_R of size $R \times R$ and zero-matrix $\mathbf{0}_{M-R}$ of size $R \times (M - R)$. In the sequel, $(\cdot)^H$ denotes the Hermitian and $(\cdot)^{-1}$ the inverse of a matrix. The underlying observation matrix of the system model is given by

$$\mathbf{C}(k) = \mathbf{F}_M \mathbf{Q}_R \mathbf{Q}_R^H \mathbf{F}_M^{-1} \mathbf{X}(k). \quad (4)$$

With these definitions, the *diagonalized* Kalman equations result in

$$\mathbf{K}(k) = \mathbf{P}(k) \mathbf{X}^H(k) \left(\mathbf{X}(k) \mathbf{P}(k) \mathbf{X}^H(k) + \frac{M}{R} \boldsymbol{\Psi}_{ss}(k) \right)^{-1} \quad (5a)$$

$$\mathbf{E}(k) = \mathbf{F}_M \mathbf{Q}_R \left(\mathbf{y}_R(k) - \mathbf{Q}_R^H \mathbf{F}_M^{-1} \mathbf{X}(k) \hat{\mathbf{W}}(k) \right) \quad (5b)$$

$$\hat{\mathbf{W}}^+(k) = \hat{\mathbf{W}}(k) + \mathbf{K}(k) \mathbf{E}(k) \quad (5c)$$

$$\mathbf{P}^+(k) = \left(\mathbf{I}_M - \frac{R}{M} \mathbf{K}(k) \mathbf{X}(k) \right) \mathbf{P}(k) \quad (5d)$$

$$\hat{\mathbf{W}}(k+1) = A \cdot \hat{\mathbf{W}}^+(k) \quad (5e)$$

$$\mathbf{P}(k+1) = A^2 \cdot \mathbf{P}^+(k) + \boldsymbol{\Psi}_{\Delta\Delta}(k), \quad (5f)$$

with $\mathbf{X}(k) = \text{diag}\{\mathbf{F}_M \cdot \mathbf{x}_M(k)\}$ and forgetting factor A . The estimate of the transfer function is denoted by

$$\hat{\mathbf{W}}(k) = \mathbf{F}_M \begin{pmatrix} \hat{\mathbf{w}}_{M-R+1}(kR) \\ \mathbf{0}_{R-1} \end{pmatrix} \quad (6)$$

of size $M \times 1$ with $\hat{\mathbf{w}}_{M-R+1}(kR)$ defined analogously to (1). The column vector $\mathbf{0}_{R-1}$ contains $R - 1$ zeros. After each update the estimate $\hat{\mathbf{W}}$ is restricted by zeroing the last $R - 1$ coefficients in the time domain. This constraint is necessary to prevent cyclic artifacts in the overlap-save framework used. The $M \times M$ matrices $\mathbf{P}(k)$ and $\mathbf{K}(k)$ are the estimates of the covariance matrix of the estimation error and the Kalman gain, respectively. $\boldsymbol{\Psi}_{ss}(k)$ and $\boldsymbol{\Psi}_{\Delta\Delta}(k)$ denote the covariance matrices of the measurement noise and process noise, respectively. In the actual implementation the covariance matrices are approximated by diagonalized estimates (see [17], [18] for more details).

2.1. Influence of Signal Correlation on System Identification

This section deals with the question whether the correlation properties of the excitation signal degrade the performance of the Kalman filter adaptation. For this purpose, the logarithmic system distance

$$\text{SysDis}(i) [\text{dB}] = 10 \lg \left(\frac{\|\mathbf{w}(i) - \hat{\mathbf{w}}(i)\|^2}{\|\mathbf{w}(i)\|^2} \right) \quad (7)$$

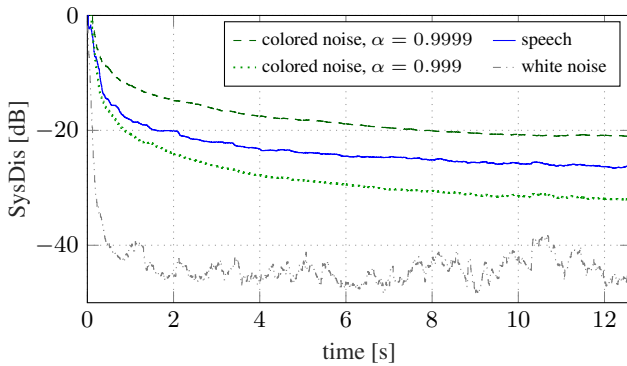


Fig. 2. System identification with different excitation signals $x(i)$ ($s(i)$: white noise, SNR = 30 dB, $\mathbf{w}_{\text{slow}}(i)$)

is introduced. Figure 2 depicts the results for various excitation signals with different correlation properties. For the comparison, a speech signal, white Gaussian noise and two colored noise signals have been considered. The colored noise relies on a first order autoregressive model with different feedback factors α . For the simulations slowly time variant impulse responses $\mathbf{w}_{\text{slow}}(i)$ of length 192 (sampling rate 8 kHz) have been used, which were generated according to [20]. The underlying measurements for the results of Fig. 2 and 4 were carried out in an empty soundproof booth. The parameters for the Kalman filter were set to $M = 256$, $R = 64$ and $A = 1$. At the microphone an SNR of 30 dB between the system response and a white Gaussian measurement noise was adjusted.

Figure 2 demonstrates that the adaptation performance depends on the properties of the excitation signal. Although the Kalman filter takes into account a certain amount of correlation via an automatic adaptive stepsize control mechanism, a more uncorrelated excitation signal obviously results in better performance in terms of convergence speed and steady-state behaviour. As a result in the sequel, a decorrelation stage is introduced for an improved Kalman filter design.

3. REFERENCE MODEL: DECORRELATION VIA LINEAR PREDICTION

In this section, the effect of a decorrelation prior to the adaptation and transmission is analyzed. Therefore, in a first step a reference model according to Fig. 3 is introduced. The excitation signal $x(i)$ is

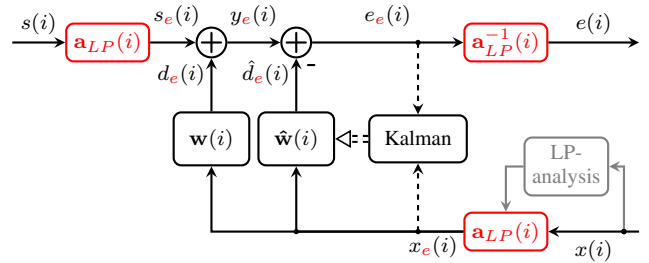


Fig. 3. Reference model

spectrally whitened applying linear prediction (LP) techniques [21]. For this principle experiment the prediction is performed every 20 ms on the next 20 ms of the excitation signal. An FIR filter with the impulse response $\mathbf{a}_{LP}(i) = (a_0(i), a_1(i), \dots, a_P(i))^T$ performs the actual decorrelation with prediction degree P , so that the residual

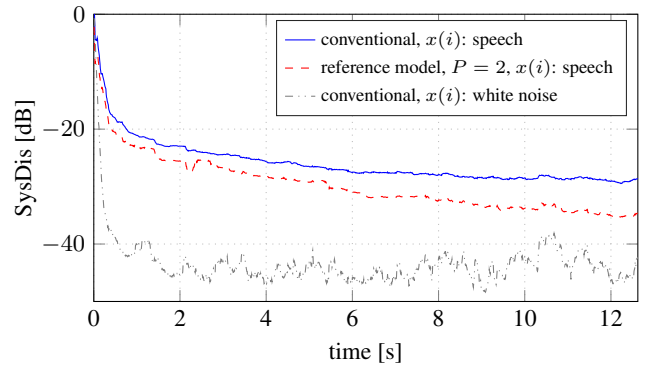


Fig. 4. Comparison of conventional Kalman algorithm and reference model ($s(i)$: white noise, SNR = 30 dB, $\mathbf{w}_{\text{slow}}(i)$)

signal $x_e(i)$ is spectrally whitened as described in [21]. The same prediction filter is used for measurement noise $s(i)$. As a result, the reference model can also be interpreted as a conventional Kalman algorithm running in the “residual signal domain”. The simulations were performed with the system parameters as specified in Sec. 2.1. The prediction degree is set to $P = 2$ as numerous experiments verified that in most cases this prediction degree is sufficient. Figure 4 shows the effect of the linear prediction filters. Even though the results of white noise excitation cannot be achieved, the reference model results in significant improvements of several dB.

Obviously, the reference model in this structure is not realizable, since in real applications, e.g., AEC, a residual signal $x_e(i)$ cannot be applied as excitation, the measurement noise $s(i)$ is not particularly available, and a delay due to the LP-analysis should be avoided. In order to derive an appropriate realizable structure, the physical transmission and the adaptation process are decoupled in analogy to ideas presented in [6, 7, 9] for the NLMS-algorithm in the time domain. In the next section, this idea will be adapted and generalized for the Kalman algorithm in the frequency domain.

4. KALMAN ALGORITHM WITH DECORRELATION

The principle idea of decoupling of adaptation and transmission is to shift the decorrelation filters $\mathbf{a}_{LP}(i)$ in Fig. 3 into the adaptation paths as depicted in Fig. 5.

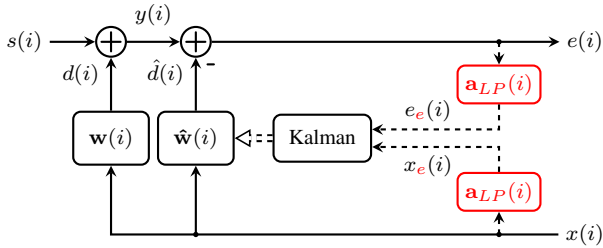


Fig. 5. Kalman filter with decorrelation in the adaptation paths

A system theoretical analysis shows that the required shifting of the LP-filter from the “ $s(i)$ -path” and subsequent swapping with $\mathbf{w}(i)$ and $\hat{\mathbf{w}}(i)$ causes principal errors due to the time variance of the involved filters. While in case of $\mathbf{w}(i)$ the error due to the swapping is relatively small, and turned out to be irrelevant for practical applications, the introduced error due to the time variance of $\hat{\mathbf{w}}(i)$ affects the adaptation process notably. This error can be compensated by introducing a refiltering stage in the adaptation paths as described in [9]. The aim of this stage is to refilter the signals $x(i)$ and $e(i)$ in such a way that they only depend on one set of prediction coefficients $\mathbf{a}_{LP}(i)$ and on the current filter coefficients $\hat{\mathbf{w}}(i)$. As a result, system theoretically the filters $\mathbf{a}_{LP}(i)$ and $\hat{\mathbf{w}}(i)$ can be exchanged. The corresponding principal block diagram of the new structure is illustrated in Fig. 6.

For the decorrelation and refiltering of the excitation signal $x(i)$, the matrix

$$\mathbf{x}_{\text{states}}(k) = \begin{pmatrix} x(kR - M + 1) & \cdots & x(kR - M - P + 1) \\ \vdots & & \vdots \\ x(kR) & \cdots & x(kR - P) \end{pmatrix}$$

which contains the filter states of the decorrelation filter $\mathbf{a}_{LP}(kR)$ for the last M time instances, is defined. The decorrelation and refiltering

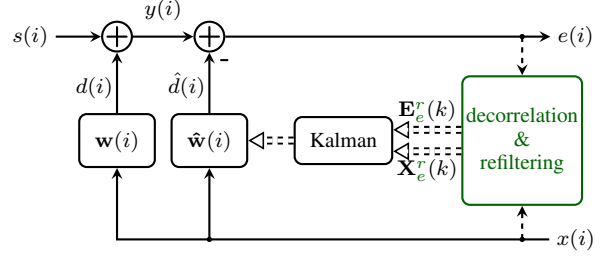


Fig. 6. Kalman filter with decorrelation and refiltering

of $x(i)$ can now be formulated in the frequency domain according to

$$\mathbf{X}_e^r(k) = \text{diag} \{ \mathbf{F}_M \cdot \mathbf{x}_{\text{states}}(k) \cdot \mathbf{a}_{LP}(kR) \}. \quad (8)$$

In comparison to $\mathbf{X}_e(k) = \text{diag} \{ \mathbf{F}_M \cdot \mathbf{x}_e(k) \}$, which can depend on different sets of coefficients $\mathbf{a}_{LP}(i)$, the signal $\mathbf{X}_e^r(k)$ depends only on the current coefficients $\mathbf{a}_{LP}(kR)$. Starting from (5b) and adding the decorrelation filtering in the frequency domain expressed by multiplication with $\mathbf{F}_M \mathbf{Q}_R \mathbf{Q}_R^H \mathbf{F}_M^{-1} \mathbf{A}_{LP}(k)$, the decorrelation and refiltering of the error signal $\mathbf{E}(k)$ can be calculated by

$$\mathbf{E}_e^r(k) = \mathbf{F}_M \mathbf{Q}_R \mathbf{Q}_R^H \mathbf{F}_M^{-1} \mathbf{A}_{LP}(k) \mathbf{F}_M \mathbf{Q}_{R+P} (\mathbf{y}_{R+P}(k) - \mathbf{Q}_{R+P}^H \mathbf{F}_M^{-1} \mathbf{X}(k) \hat{\mathbf{W}}(k)). \quad (9)$$

Here, the matrix

$$\mathbf{A}_{LP}(k) = \text{diag} \left\{ \mathbf{F}_M \begin{pmatrix} \mathbf{a}_{LP}(kR) \\ \mathbf{0}_{M-P-1} \end{pmatrix} \right\} \quad (10)$$

represents the transfer function of the decorrelation filter, with $\mathbf{0}_{M-P-1}$ being a column vector containing $M - P - 1$ zeros. Vector $\mathbf{y}_{R+P}(k)$ and matrix \mathbf{Q}_{R+P} are defined analogically to (3) and to \mathbf{Q}_R , respectively. In (9) $R + P$ values $\mathbf{y}_{R+P}(k)$ have to be used in contrast to R values in (5b). This is because P additional values of the error signal are needed as refiltered decorrelation filter states. After performing the cyclic convolution in the frequency domain, by multiplying with $\mathbf{A}_{LP}(k)$, R valid values can be obtained. This also leads to the constraint that the impulse response of the adaptive filter $\hat{\mathbf{w}}(k)$ has to be of length $M - R - P + 1$, so that the cyclic corruption caused by filtering in the frequency domain is short enough to yield $R + P$ correct values.

If the decorrelated and refiltered quantities from (8) and (9) are used instead of $\mathbf{X}(k)$ and $\mathbf{E}(k)$, the *diagonalized* Kalman equations with decorrelation

$$\mathbf{K}(k) = \mathbf{P}(k) \mathbf{X}_e^r H(k) \left(\mathbf{X}_e^r(k) \mathbf{P}(k) \mathbf{X}_e^r H(k) + \frac{M}{R} \Psi_{ss}(k) \right)^{-1} \quad (11a)$$

$$\hat{\mathbf{W}}^+(k) = \hat{\mathbf{W}}(k) + \mathbf{K}(k) \mathbf{E}_e^r(k) \quad (11b)$$

$$\mathbf{P}^+(k) = \left(\mathbf{I}_M - \frac{R}{M} \mathbf{K}(k) \mathbf{X}_e^r(k) \right) \mathbf{P}(k) \quad (11c)$$

$$\hat{\mathbf{W}}(k+1) = A \cdot \hat{\mathbf{W}}^+(k) \quad (11d)$$

$$\mathbf{P}(k+1) = A^2 \cdot \mathbf{P}^+(k) + \Psi_{\Delta\Delta}(k) \quad (11e)$$

can be derived. The observation matrix

$$\mathbf{C}_e^r(k) = \mathbf{F}_M \mathbf{Q}_R \mathbf{Q}_R^H \mathbf{F}_M^{-1} \mathbf{A}_{LP}(k) \cdot \mathbf{F}_M \mathbf{Q}_{R+P} \mathbf{Q}_{R+P}^H \mathbf{F}_M^{-1} \mathbf{X}(k)$$

is effective. Comparing $\mathbf{C}_e^r(k)$ with (4) shows that the new observation matrix can be interpreted as a concatenation of a

physically observable part $\mathbf{F}_M \mathbf{Q}_{R+P} \mathbf{Q}_{R+P}^H \mathbf{F}_M^{-1} \mathbf{X}(k)$ and a part $\mathbf{F}_M \mathbf{Q}_R \mathbf{Q}_R^H \mathbf{F}_M^{-1} \mathbf{A}_{LP}(k)$ that describes the decorrelation.

In contrast to the reference model in Fig. 3, where the prediction was performed every 20 ms on the next 20 ms of the excitation signal, the prediction in the refiltered case has to be performed on the last M samples every R samples to ensure that the prediction is performed on the relevant samples. As positive side effect, the prediction causes no algorithmic delay and is adapted for each frame.

4.1. Complexity Figures

The Kalman filter with decorrelation according to Fig. 6 requires an additional LP-analysis, decorrelation, and refiltering in the adaptation paths for each block. The LP-analysis is performed on a frame of M samples with frameshift R and prediction order P . Equation (8) comprises the decorrelation operations (with an inherent refiltering) performed in the lower adaptation path. Thus, additional complexity originates from the matrix multiplication $\mathbf{x}_{states}(k) \cdot \mathbf{a}_{LP}(kR)$ which consists of $M \cdot P$ real multiplications and $M \cdot P$ real additions. For the increase of complexity in the upper adaptation path, (9) has to be compared to (5b). The decorrelation in (9) is calculated by $\mathbf{F}_M \mathbf{Q}_R \mathbf{Q}_R^H \mathbf{F}_M^{-1} \mathbf{A}_{LP}(k)$. Hence, one FFT, one IFFT and M complex multiplications are needed. The refiltering is performed by taking P additional differences (within the brackets of (9)) into account. Concludingly, in the underlying simulation examples the complexity increases in an order of 20 to 25 %.

5. SIMULATION RESULTS

Simulations were carried out to evaluate the effect of the proposed decorrelation and refiltering method in an AEC application in terms of logarithmic system distance. Besides the time variant, stationary impulse responses $\mathbf{w}_{slow}(i)$ (see Sec. 2.1) for the simulations also strongly time variant impulse responses $\mathbf{w}_{fast}(i)$ have been applied. The corresponding measurements for $\mathbf{w}_{fast}(i)$ were performed with a person moving between loudspeaker and microphone in the sound-proof booth. As a time variance indication (TVI) of $\mathbf{w}_{slow}(i)$ or $\mathbf{w}_{fast}(i)$, respectively, the logarithmic system distance between successive impulse responses is utilized. The parameters of the Kalman filter are set to $M = 256$, $R = 64$ and $P = 2$.

Figure 7 shows the results for a far-end single talk scenario (i.e., $x(i)$: speech, $s(i)$: white noise) with the slowly time variant impulse responses $\mathbf{w}_{slow}(i)$. In order to choose realistic “best case” conditions for the AEC, the simulations were performed for two different

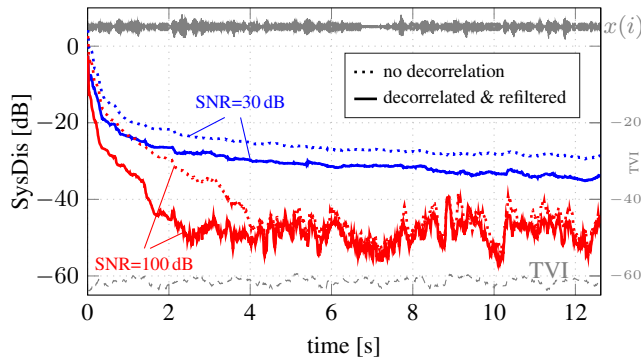


Fig. 7. Comparison of conventional Kalman algorithm with new approach including LP filtering. ($x(i)$: speech, $s(i)$: white noise, $A = 1$ for SNR = 30 dB and $A = 0.99995$ for SNR = 100 dB, $\mathbf{w}_{slow}(i)$)

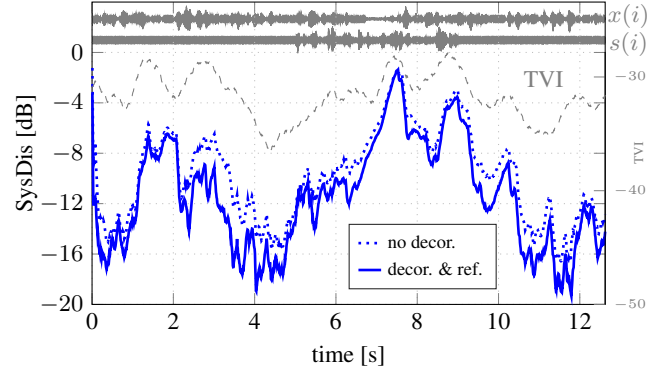


Fig. 8. Comparison of conventional Kalman algorithm with new approach including LP filtering. ($x(i)$: far-end speech, $s(i)$: near-end speech, $A = 0.995$, SNR = 0 dB in double talk periods, SNR = 40 dB in single talk periods, $\mathbf{w}_{fast}(i)$)

SNR values of 30 dB (—) and 100 dB (—) at the microphone. At an SNR of 30 dB the decorrelation leads to an improvement in system distance of approximately 5 dB. At an SNR of 100 dB especially the improvement in convergence speed can be observed. The corresponding steady state performance is obviously limited by the time variance of the impulse responses $\mathbf{w}_{slow}(i)$.

Figure 8 summarizes the results for a “worst case” condition, i.e., a double talk scenario ($x(i)$, $s(i)$: speech) with strongly time variant impulse responses $\mathbf{w}_{fast}(i)$. It can be observed that the logarithmic system distance follows to a certain extent the course of the TVI leading to misalignments, e.g., at the time instance of 7.5 s. Nevertheless, even under these severe conditions both Kalman algorithms show stable performance. In comparison, the new approach with LP filters outperforms the conventional Kalman algorithm and provides an improvement in system distance of up to 3 dB.

The results clearly indicate that even in case of a Kalman filter based adaptation correlation affects the identification process and that the introduction of LP filters leads to an attractive solution to address this problem.

6. CONCLUSION

In this paper a decorrelation method based on linear prediction was reviewed and adapted to Kalman filter based adaptation, working blockwise in the frequency domain. Within some principal experiments, it has been shown that a decorrelation of the excitation signal improves the identification performance. The introduction of a reference model proved the effectiveness of spectrally whitened excitation signals produced by linear prediction techniques. Motivated by the promising results, a new Kalman filter based approach including linear prediction filters was derived. Simulation results for an acoustic echo cancellation application show improvements in term of convergence speed and steady-state behaviour. Depending on the simulation conditions, gains in an order of 5 dB can be achieved. With respect to a gain/complexity tradeoff it is of interest that these gains can be obtained taking only a reasonable increase of complexity into account.

In the next step we extend our new concept to multi-channel systems, where besides the autocorrelation also the cross-correlation between the channels is of interest. The question is, to which extent the linear prediction can improve the correlation properties of the excitation signals, to counteract the non-uniqueness problem of multi-channel system identification.

7. REFERENCES

- [1] S. Haykin, *Adaptive filter theory*, Pearson Education India, 2008.
- [2] S.L. Gay and J. Benesty, Eds., *Acoustic Signal Processing for Telecommunication*, Kluwer Academic Publishers, 2000.
- [3] J. Benesty, T. Gänslér, D.R. Morgan, M. Sondhi, and S.L. Gay, *Advances in Network and Acoustic Echo Cancellation*, Digital Signal Processing. Springer-Verlag, 2001.
- [4] E. Hänsler and G. Schmidt, *Acoustic Echo and Noise Control – A Practical Approach*, John Wiley & Sons, 2004.
- [5] E. Hänsler and G. Schmidt, Eds., *Topics in Acoustic Echo and Noise Cancellation*, Springer-Verlag, 2006.
- [6] C. Antweiler and P. Vary, “Combined implementation of predictive speech coding and acoustic echo cancellation,” in *Proc. of the European Signal Processing Conference (EUSIPCO)*, Brüssel, Aug. 1992, pp. 1641–1644.
- [7] C. Antweiler and A. Schmitz, “Acoustic echo control combined with two orthogonalizing techniques,” in *Proc. of European Signal Processing Conference (EUSIPCO)*, Edinburgh, Sep. 1994, pp. 1748–1751.
- [8] M. Mboup, M. Bonnet, and N. Bershad, “LMS coupled adaptive prediction and system identification: a statistical model and transient mean analysis,” *IEEE Transactions on Signal Processing*, vol. 42, no. 10, pp. 2607–2615, Oct. 1994.
- [9] C. Antweiler, *Orthogonalisierende Algorithmen für die digitale Kompensation akustischer Echos*, Ph.D. thesis, RWTH Aachen University, 1995.
- [10] S. Gazor and T. Liu, “Adaptive filtering with decorrelation for coloured AR environments,” *IEE Proceedings - Vision, Image and Signal Processing*, vol. 152, no. 6, pp. 806–818, Dec. 2005.
- [11] M. Rotaru, F. Albu, and H. Coanda, “A variable step size modified decorrelated NLMS algorithm for adaptive feedback cancellation in hearing aids,” *Proc. of ISETC*, vol. 2012, pp. 263–266, 2012.
- [12] K. Ozeki and T. Umeda, “An adaptive filtering algorithm using an orthogonal projection to an affine subspace and its properties,” *Electronics and Communications in Japan (Part I: Communications)*, vol. 67, no. 5, pp. 19–27, 1984.
- [13] P. C. W. Sommen and C. J. van Valburg, “Efficient realisation of adaptive filter using an orthogonal projection method,” in *Proc. of International Conference on Acoustics, Speech, and Signal Processing (ICASSP)*, May 1989, pp. 940–943 vol.2.
- [14] M. Rupp, “A comparison of gradient-based algorithms for echo compensation with decorrelating properties,” in *Proc. of IEEE Workshop on Applications of Signal Processing to Audio and Acoustics (WASPAA)*, Oct. 1993, pp. 12–15.
- [15] C. Paleologu, J. Benesty, and S. Ciochină, “Study of the general Kalman filter for echo cancellation,” *IEEE Transactions on Audio, Speech and Language Processing*, vol. 21, no. 8, pp. 1539–1549, Aug. 2013.
- [16] C. Paleologu, J. Benesty, S. Ciochină, and S.L. Grant, “A Kalman filter with individual control factors for echo cancellation,” in *Proc. of IEEE International Conference on Acoustics, Speech, and Signal Processing (ICASSP)*, May 2014, pp. 5974–5978.
- [17] G. Enzner and P. Vary, “Frequency-domain adaptive Kalman filter for acoustic echo control in hands-free telephones,” *Signal Processing*, vol. 86, no. 6, pp. 1140–1156, 2006.
- [18] G. Enzner, *A Model-based Optimum Filtering Approach to Acoustic Echo Control: Theory and Practice*, Ph.D. thesis, RWTH Aachen University, 2006.
- [19] D. P. Mandic, S. Kanna, and A. G. Constantinides, “On the intrinsic relationship between the least mean square and Kalman filters [lecture notes],” *IEEE Signal Processing Magazine*, vol. 32, no. 6, pp. 117–122, Nov. 2015.
- [20] C. Antweiler and H. G. Symanzik, “Simulation of time variant room impulse responses,” in *Proc. of IEEE International Conference on Acoustics, Speech, and Signal Processing (ICASSP)*, May 1995, vol. 5, pp. 3031–3034.
- [21] P. Vary and R. Martin, *Digital Speech Transmission: Enhancement, Coding and Error Concealment*, John Wiley & Sons, 2006.